

## Using hard-x-ray photoelectron spectroscopy to measure the oxidation state of gated Co/AlO<sub>x</sub> interfaces

Cristina Balan,<sup>1</sup> Johanna Fischer,<sup>2</sup> Capucine Gueneau,<sup>2</sup> Aymen Fassatoui,<sup>1</sup> Jean-Pascal Rueff,<sup>3,4</sup> Denis Ceolin,<sup>3</sup> Maurizio De-Santis,<sup>1</sup> Jan Vogel,<sup>1</sup> Laurent Ranno,<sup>1</sup> H el ene B ea,<sup>2,5</sup> and Stefania Pizzini<sup>1,\*</sup>


<sup>1</sup>*Universit  Grenoble Alpes, CNRS, Institut N el, Grenoble 38042, France*

<sup>2</sup>*Universit  Grenoble Alpes, CNRS, CEA, SPINTEC, Grenoble 38054, France*

<sup>3</sup>*Synchrotron SOLEIL, L'Orme des Merisiers, Saint-Aubin, Gif-sur-Yvette 91192, France*

<sup>4</sup>*Laboratoire de Chimie Physique - Mati re et Rayonnement (LCPMR), Sorbonne Universit , CNRS, Paris 75005, France*

<sup>5</sup>*Institut Universitaire de France (IUF), France*

 (Received 11 February 2024; revised 26 April 2024; accepted 17 May 2024; published 11 June 2024)

The perpendicular magnetic anisotropy (PMA) of metal/ferromagnet (FM)/oxide trilayers is known to depend on the degree of oxidation of the FM/oxide interface. Among the different methods to tune the PMA, magnetoionics is emerging as a promising technique with potential applications in low-power spintronic devices. In this work, the PMA of Pt/Co/AlO<sub>x</sub>/HfO<sub>2</sub> capacitorlike devices was gradually tuned by electric field gating. Hard-x-ray photoelectron spectroscopy (HAXPES) measurements at a synchrotron radiation source, guaranteeing tunable photon energies, a collimated beam, and a large photon flux, have allowed us to probe the composition of the cobalt ultrathin film buried below the dielectric layer of the capacitors, and its evolution upon the application of the gate voltage. The Co 2*p* HAXPES spectra of the gated devices were compared to those obtained for Pt/Co/AlO<sub>x</sub> reference samples, for which the PMA was controlled by tuning the Co oxidation with oxygen plasma. For similar magnetic anisotropy states, the two types of samples exhibit equivalent Co 2*p* HAXPES spectra, with the same weight of metallic Co and CoO signatures. These results constitute direct experimental proof that, in our integrated devices, the gate voltage modifies the PMA through the modification of the oxidation state of the buried cobalt layer driven by oxygen-ion migration.

DOI: [10.1103/PhysRevApplied.21.064023](https://doi.org/10.1103/PhysRevApplied.21.064023)

### I. INTRODUCTION

The manipulation of interfacial magnetic anisotropy via the gate voltage is a promising route towards the realization of low-power spintronic devices [1,2]. In ferromagnetic (FM) ultrathin films, the electric field can tune the perpendicular magnetic anisotropy (PMA) either by electronic effects [2–5] or by magnetoionic effects when the dielectric layer acts also as an ionic conductor. In the latter case, the gate voltage can drive the migration of ions (oxygen [6,7], hydrogen [8,9], lithium [10], nitrogen [11]) across a dielectric layer and towards the FM interface, leading to nonvolatile modifications of the sample composition and, consequently, of the magnetic properties, and in particular the PMA. The aim of this work is to demonstrate that in Pt/Co/AlO<sub>x</sub>/HfO<sub>2</sub> capacitorlike devices the migration of oxygen ions is at the origin of the strong nonvolatile variation of the magnetic anisotropy observed after gating [12–14].

In Pt/Co/oxide layers, the PMA at the Co/oxide interface can be as large as that found at the Pt/Co interface [15]. This anisotropy results from the hybridization of oxygen and Co electronic orbitals across the interface [1,16] and depends on the degree of oxidation of the Co layer. The dependence of the interfacial anisotropy constant ( $K_s^{\text{ox}}$ ) as a function of the oxidation of the Co/oxide interface has a characteristic bell-like shape, with a maximum for the optimal oxidation conditions obtained when the Co—O bonds prevail over Co—*M* bonds [16–19]. This explains why oxygen-ion migration is invoked whenever the PMA is tuned in a nonvolatile way with a gate voltage [6,7,12–14,20].

Clear experimental proof of the correlation between the gate-induced evolution of PMA and the degree of oxidation of an ultrathin ferromagnetic layer buried under the dielectric layer of a solid-state capacitorlike device, measured for the same device, is still missing. The surface sensitivity and limited photon flux of laboratory x-ray photoemission spectroscopy does not allow such observations on realistic devices. On the other

\*Corresponding author: [stefania.pizzini@neel.cnrs.fr](mailto:stefania.pizzini@neel.cnrs.fr)

hand, hard-x-ray photoelectron spectroscopy (HAXPES) measurements at a synchrotron radiation source [21] guarantee tunable photon energy, a collimated beam, and a large photon flux. Moreover, since the penetration depth of x-rays, as well as the escape depth of photoelectrons, increases with the x-ray energy, HAXPES is the ideal technique to probe, with a good signal-to-noise ratio (SNR), the electronic structure of ultrathin layers below thick dielectric layers.

Our results clearly demonstrate that the modification of the easy magnetization axis from in plane (IP) to out of plane (OOP) and then to a paramagnetic (PM) state, as the negative gate potential is increased, corresponds to the gradual modification of the Co layer from metal-like to CoO-like. To strengthen our conclusions, the Co 2*p* HAXPES spectra of the devices were compared to those obtained for Pt/Co/AIO<sub>x</sub> reference samples, for which the PMA was controlled by tuning the Co oxidation by oxygen plasma. For similar magnetic anisotropy states, the two types of samples exhibit equivalent spectra, with the same weights of metallic cobalt and CoO signatures. These results constitute direct experimental proof that, in our integrated devices, the gate voltage modifies the PMA through the modification of the oxidation state of the buried cobalt layer driven by oxygen-ion migration.

## II. MAGNETIC PROPERTIES OF REFERENCE AND CAPACITORLIKE DEVICES

A Pt(3)/Co(0.46–0.87)/Al(1.9–2.56) trilayer film (thicknesses in nm) was deposited by magnetron sputtering on a 4-inch Si/SiO<sub>2</sub> substrate. The Co and Al layers form a double wedge with thickness gradients deposited perpendicular to each other [see Fig. 1(a)]. The stack was then oxidized for 40 s in an oxygen plasma (10 W,  $3 \times 10^{-3}$  mbar). The Al thickness gradient leads to a variation of the degree of oxidation of the Co/Al interface and of the Co layer along the Al wedge and, as a consequence, to a change of the interfacial magnetic anisotropy. This is illustrated in Fig. 1(a), which shows the remanent magnetization measured by scanning polar magneto-optical Kerr effect (MOKE) magnetometry. This map allows us to highlight the sample regions with OOP magnetization [areas with optimum oxidation, in orange in Fig. 1(a)] together with the transitions towards in-plane magnetization (for thicker Al layers, i.e., underoxidized Co layer) and to the paramagnetic state (for thin Al layers, where Co is overoxidized). This is the general behavior found in the literature for Pt/FM/oxide (FM corresponds to Co, Co-Fe-B, etc.) trilayers where FM oxidation is gradually increased [16–19].

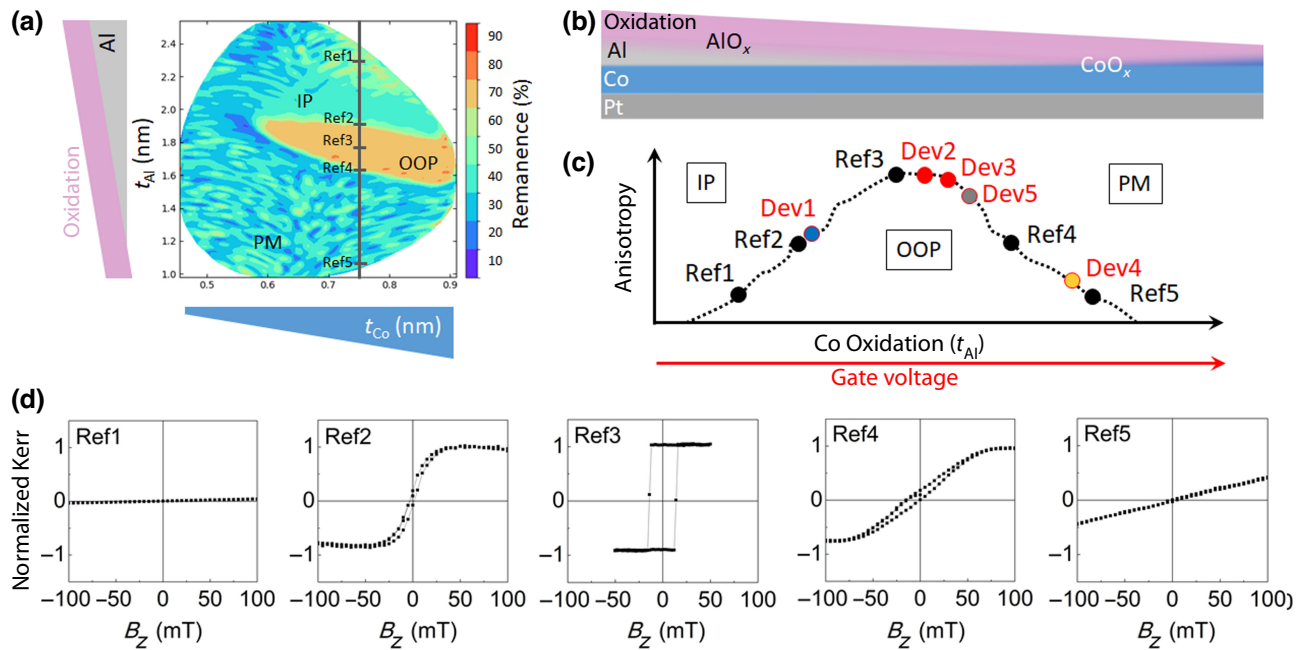


FIG. 1. (a) Remanent magnetization measured by polar MOKE on the Pt/Co/AIO<sub>x</sub> double wedge, with Co and Al thickness gradients and oxidized by oxygen plasma. Central region (orange) shows OOP magnetization; underoxidized Co region with larger Al thickness has IP magnetization; overoxidized Co region with thin Al layers is paramagnetic. (b) Sketch of the Pt/Co/AIO<sub>x</sub> stack used for the reference samples; aluminum layer was oxidized with oxygen plasma in the deposition chamber. (c) Sketch illustrating the variation of magnetic anisotropy with the oxidation rate of the Co layer (based on results reported in Ref. [17]) and the approximate position of reference samples (points in blue) and gated devices (red points) on the curve. (d) Hysteresis loops measured by polar MOKE for Ref1–Ref5.

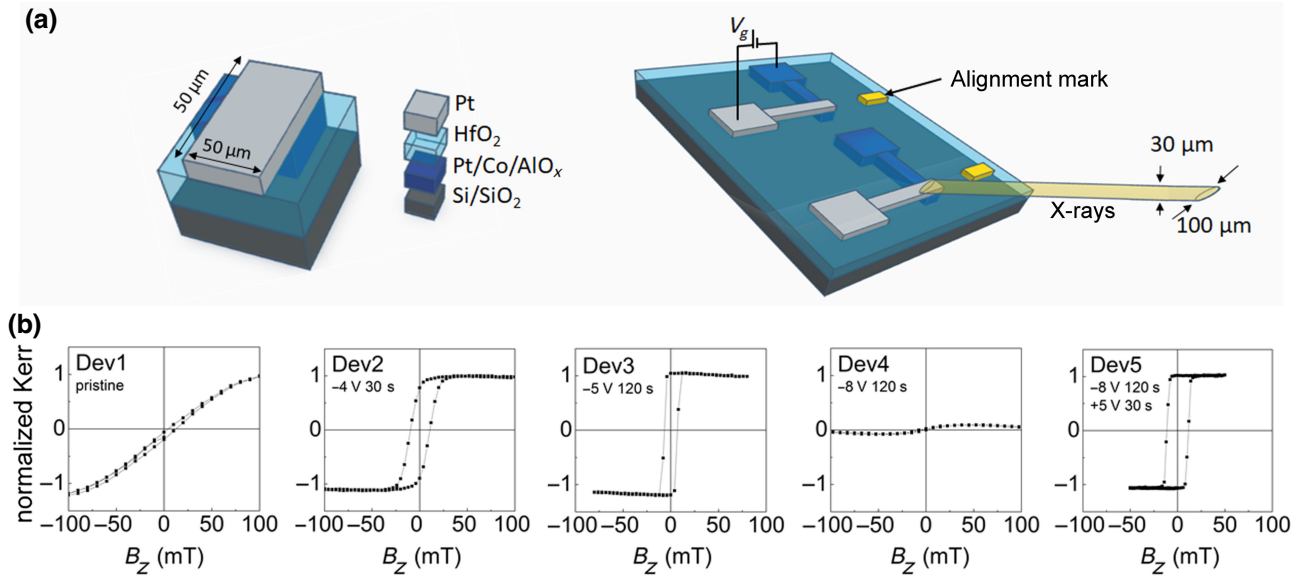


FIG. 2. (a) Sketch of the capacitorlike devices together with the geometry of the HAXPES measurements. (b) Hysteresis loops of capacitorlike devices Dev1–Dev5. Approximate anisotropy of the devices based on the shape of the hysteresis loop and on HAXPES data is shown in Fig. 1(c).

For the present study, we have selected Pt/Co/AlO<sub>x</sub> reference samples with a fixed Co thickness of 0.75 nm and five Al thicknesses (2.3, 1.9, 1.75, 1.6, and 1.1 nm) with increasing oxidation of the Co layer, which we refer to as Ref1, Ref2, Ref3, Ref4, and Ref5, respectively. Ref1 is in the IP magnetization area, Ref2 is close to the transition between IP and OOP, Ref3 is in the OOP region, Ref4 is close to the transition between OOP and PM, and Ref5 is in the PM region. In Ref1 and Ref2, Co is underoxidized; in Ref3, Co is close to the optimum oxidation for PMA; in Ref4 and Ref5, Co is overoxidized. A sketch illustrating the variation of the magnetic anisotropy in the reference samples is shown in Fig. 1(c), together with the hysteresis loops measured by MOKE magnetometry in Fig. 1(d).

Pt/Co(0.75)/Al(1.9)O<sub>x</sub> trilayers with compositions close to that of Ref2, i.e., near the IP-OOP magnetic transition in an underoxidized state, were micropatterned as capacitorlike devices. A 5-nm-thick high-*k* HfO<sub>2</sub> dielectric layer was deposited by atomic layer deposition on top of a network of Pt/Co/AlO<sub>x</sub> strips processed by UV lithography and lift-off (see Refs. [12,13] for more details on the preparation methods). 50 × 50-μm<sup>2</sup> 3-nm-thick Pt electrodes, acting as local gates, were then patterned on top on the magnetic strips [see Fig. 2(a)]. Five capacitorlike devices were studied. In the first one (Dev1), the Pt/Co/AlO<sub>x</sub> stack was left in the as-prepared (pristine) state, while the magnetic anisotropies of Dev 2, Dev3, and Dev4 were tuned with increasingly negative voltages. Dev5 was gated with the same negative voltage as Dev4, followed by a positive voltage. The gating processes are described in Table I.

The hysteresis loops of the devices were measured by polar MOKE in the region below the Pt electrodes. Before gating, all the loops show typical S-like shapes with zero remanence, similar to that obtained for reference sample Ref2 [shown in Fig. 2(b) for Dev1]. After gating, the shape of the loops of Dev2–Dev5 reveal that the magnetic anisotropy was modified by the gate voltage. The open square loops of Dev2 and Dev3 illustrate that the application of the negative voltage increases the PMA and sets the easy magnetization axis out of plane. For larger applied voltages, the anisotropy decreases, as shown by the closed loop of Dev4. The trend in magnetic anisotropy for increasing negative voltage observed for the devices is therefore equivalent to that observed for the reference samples for increasing Co oxidation. These results then suggest that, after gating, in Dev2 and Dev3, the Co layer has been optimally oxidized, while in Dev4, where the OOP easy axis is lost, Co has been overoxidized. Dev5, which was subject to the same gating process as Dev4 and was subsequently

TABLE I. Applied gate voltage and application time for the capacitorlike devices.

Sample	Al thickness (nm)	Co thickness (nm)	$V_g$ (V)	Time (s)
Dev1	1.9	0.75	...	...
Dev2	1.9	0.75	-4	30
Dev3	1.9	0.75	-5	30
Dev4	1.9	0.75	-8	120
Dev5	1.9	0.75	-8	120
			+5	30

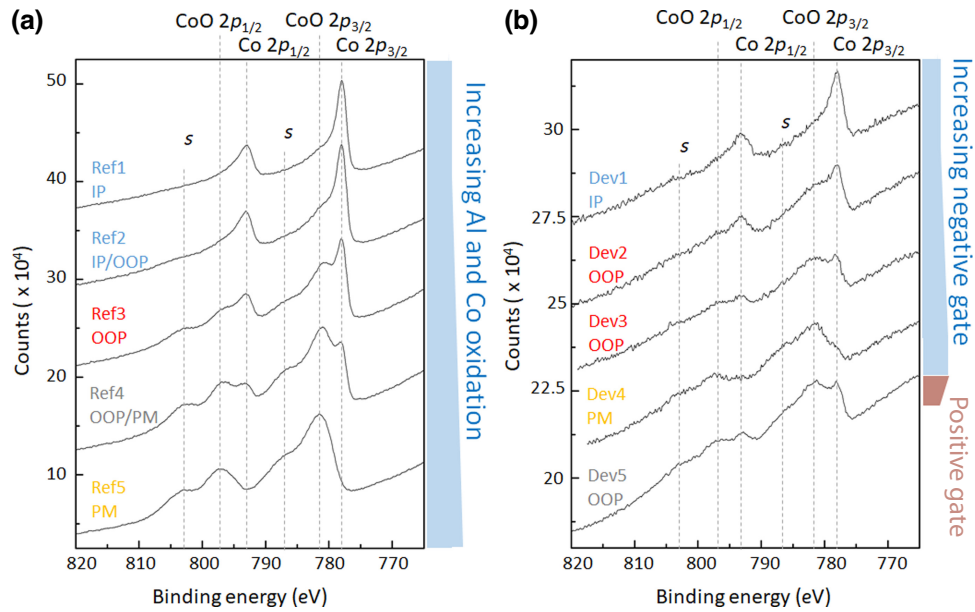


FIG. 3. Co  $2p$  HAXPES spectra of reference samples (a) and capacitorlike samples (b). To enable comparison, the spectra are shifted on the  $y$  axis.

gated with a positive voltage, recovered an open square loop. This indicates that positive voltage gating enables the Co oxidation state to decrease to recover the optimally oxidized state with an OOP easy axis. As we observed in our previous work for similar samples [12], the electric-field-induced manipulation of PMA is therefore reversible. Based on these results, Fig. 1(c) sketches the approximate magnetic anisotropy of the devices compared to that of the reference samples.

Notably, the magnetic states obtained after gating are *nonvolatile*, as they are maintained for several weeks after the removal of the electric field. This excludes electronic effects as the driving mechanism and indicates that the gate voltage drives a chemical change in the interfacial Co layer. Since  $\text{HfO}_2$  is known to be a good conductor of oxygen ions [22], our results suggest that oxygen-ion migration driven by the gate voltage is at the origin of Co oxidation, which, in turn, modifies the PMA. In this context, it should be noted (i) that the negative voltage is expected to drive the oxygen ions from the dielectric layer towards the magnetic stack and, therefore, to oxidize the Co layer; and (ii) increasing the gate voltage increases the efficiency of the magnetoionic effect by increasing exponentially the ion drift velocity [13]—more and more oxygen ions are driven towards the cobalt layer as the gate voltage is increased.

### III. EVOLUTION OF COBALT OXIDATION PROBED BY HAXPES

To confirm our interpretation of the gating effect on the PMA, we carried out HAXPES measurements at the

GALAXIES beamline of the SOLEIL synchrotron. This allowed us to compare the evolution of the composition of the Co layer in the reference samples (where the Co oxidation rate is tuned using an Al thickness gradient) and in the capacitorlike devices. The use of hard-x-ray spectroscopy was imposed by the fact that the ultrathin Co layer in the capacitorlike devices was buried below 1.9 nm of  $\text{AlO}_x$ , 5 nm of  $\text{HfO}_2$ , and 3 nm of Pt. Standard soft-x-ray photoelectron spectroscopy, with a limited electron escape depth, could therefore not be used to characterize our devices. Co  $2p$  spectra were measured using 9-keV photon energy. The size of the x-ray beam at the GALAXIES beamline is 30 (horizontal)  $\times$  100 (vertical)  $\mu\text{m}^2$  and the angle of incidence of the beam on the sample was set to  $45^\circ$ . For the capacitorlike samples, alignment marks allowed the beam to be positioned on the required device and made sure that only the gated sample area below the Pt electrodes was exposed to x-rays. The acquisition time for the reference samples was on the order of 40 min per spectrum. As expected, the SNR greatly deteriorated for the capacitorlike samples. To obtain an acceptable SNR, the Pt electrodes were removed by argon-ion beam etching. Good-quality spectra could then be measured with a total acquisition time of around 6 h per sample.

The raw Co  $2p$  spectra measured for reference samples Ref1–Ref5 and capacitorlike samples Dev1–Dev5 are shown in Figs. 3(a) and 3(b).

The evolution of the spectra of the reference samples as a function of Al layer thickness is equivalent to that previously measured with soft x-rays for a Pt/Co/ $\text{AlO}_x$  sample with constant Al thickness and increasing oxidation times [17]. The spectrum of reference sample Ref1 (largest Al

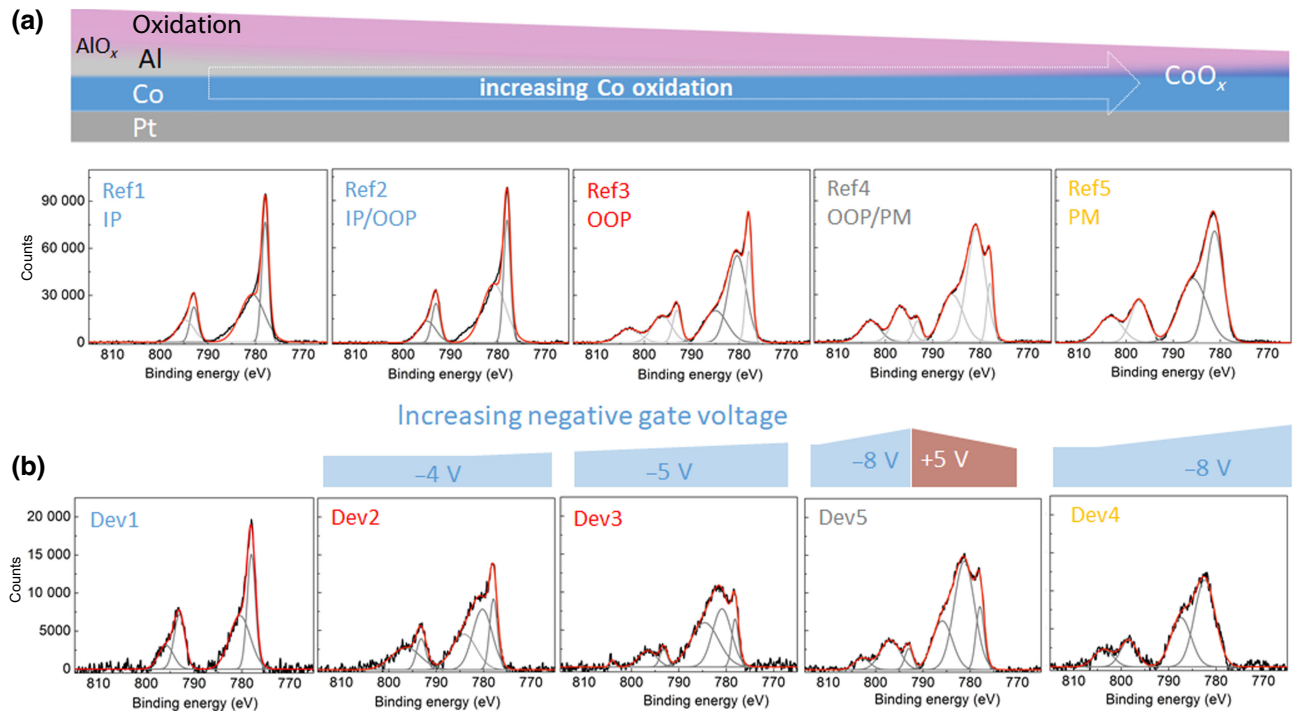


FIG. 4. Background-subtracted HAXPES data and fits using Gaussian functions for the reference samples (a) and capacitorlike samples (b). Measured spectra are in black and Gaussian peaks representing Co and CoO contributions are in gray; resulting fit is in red. Spectra are ordered according to their PMA value. Different colors in the sample designation are used to highlight the position in the anisotropy curve (IP, IP-OOP, OOP, PM) of the reference and gated samples and help the comparison.

thickness, lowest oxidation) has the features expected for pure cobalt [23,24], with Co  $2p_{1/2}$  and Co  $2p_{3/2}$  peaks lying at binding energies of 792 and 778 eV, respectively. The spectrum of reference sample Ref5 (thinnest Al layer, maximum oxidation) corresponds to pure CoO [24,25]. One can distinguish two main peaks, corresponding to CoO  $2p_{1/2}$  and CoO  $2p_{3/2}$  core levels (lying at 796 and 782 eV, respectively), and two satellite peaks (denoted  $s$  in Fig. 3 and lying at 803 and 786 eV) that arise from charge transfer between O  $2p$  and Co  $3d$  electronic levels. This charge transfer allows the coexistence of two transitions:  $2p^6d^7 \rightarrow 2p^53d^7 + e^-$  (satellite peaks) and  $2p^6d^8L \rightarrow 2p^53d^8L + e^-$  (main peaks), where  $L$  is a hole in the oxygen ligand [25]. The CoO peaks appear at larger binding energies with respect to the Co metal peaks, due to the chemical shift associated with the transfer of electrons from cobalt to oxygen. In Ref1, Co—Co bonds dominate, while the shoulder corresponding to Co—O bonds increases from Ref2 to Ref4.

The spectra of the capacitorlike devices reveal the same electronic features as the reference samples, showing that the gate voltage drives the evolution from mainly metallic Co in Dev1 (not gated) to CoO in Dev4 (gated with  $-8$  V). As expected, the spectrum of Dev1 has metallic Co character, similar to Ref2, since the pristine sample is chosen to be close to the IP-OOP transition. The presence of CoO

character increases as the negative voltage increases. The CoO shoulder is clearly seen in Dev2 and even more in Dev3, while in Dev4 the metallic contribution disappears. These results clearly show that the gate voltage acts on the PMA by oxidizing the Co layer, as in the reference samples. Since the drift velocity of the oxygen ions increases exponentially with the gate voltage [12], the oxidation of the Co layer increases upon going from Dev2 to Dev4. In Dev5, which, after gating with a negative voltage (as in Dev4), was subject to a positive voltage, the metallic Co contributions reappeared, showing that the CoO layer had been reduced. The magnetoionic effect is therefore nonvolatile and reversible.

To obtain quantitative information about the individual CoO and Co contributions to the HAXPES spectra, we have background-subtracted and fitted the spectra using Gaussian functions. The best fits are shown in Fig. 4. These data show similar evolution of the compositions of the reference and gated samples even better. Since the positions of the different spectral peaks are the same for the reference and gated samples, the electric-field-driven oxidation of the Co layer, leading to the CoO composition, is confirmed. Dev2, which has OOP magnetization, is close to Ref3; Dev3, which is still OOP, is close to Ref4 but slightly less oxidized; Dev4, which has lost the OOP easy axis, is equivalent to Ref5 and has the CoO composition. Dev5,

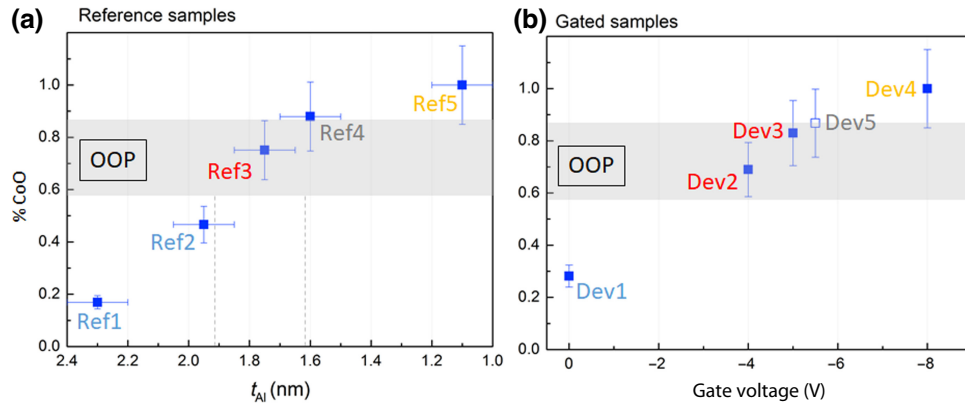


FIG. 5. Co content [corresponding to the  $\text{CoO}/(\text{Co}+\text{CoO})$  ratio] in the probed Co layer obtained from Co  $2p$  HAXPES spectra for the reference samples (a) and capacitorlike samples (b). Shaded area indicates the CoO content for which magnetization is OOP in the reference samples.

which has recovered OOP magnetization, is also close to Ref4 with a smaller CoO contribution.

The relative CoO content (i.e., the  $\text{CoO}/(\text{Co}+\text{CoO})$  ratio) in the reference and gated samples was estimated from the areas of the Co and CoO Gaussian peaks. We estimate the error bars, essentially related to the difficulty in precisely defining the background of the spectra, to be in the order of 15%. Notably, due to the limited escape depth of the photoelectrons, the contribution of different layers to the spectral weight decreases with the distance from the surface. Therefore, the technique is more sensitive to the cobalt layer closer to the surface.

The CoO content in Ref3 (maximum PMA) is around 75% and the estimated range of CoO contents in the OOP region [Al thickness between 1.9 and 1.6 nm from Fig. 1, gray region in Fig. 5(a)] is between 60% and 88%. It is interesting to note that these values are lower than those found in Ref. [17], where, in the OOP region, the CoO content varied between 82% and 98%. This is due to the higher x-ray energy used in this work (9000 eV versus 1130 eV in Ref. [17]) that leads to higher electron kinetic energies and, therefore, to a longer escape length for the electrons: using hard x-rays, the measurements are sensitive to a larger portion of the cobalt layer below the  $\text{Co}/\text{AlO}_x$  interface.

In this study, gated samples Dev2, Dev3, and Dev5 present OOP magnetization. For these devices, the CoO content lies between 70% and 87%, i.e., within the range of compositions where the reference samples also have OOP magnetization [Fig. 5(b)]. These results therefore provide direct proof that the magnetoionic effect leads to the oxidation of the Co layer via oxygen-ion migration. Moreover, since in the PMA region the relative CoO content in the gated samples and in the reference samples falls within the same range, we expect the morphology of the Co/oxide interface in the two kinds of samples to be similar.

## IV. CONCLUSIONS

The tuning of PMA by the gate voltage has often been attributed to oxygen-ion migration, but experimental proof of this effect was lacking because of the difficulty in measuring both the PMA and oxygen content in integrated solid-state devices. Our HAXPES measurements, combined with MOKE hysteresis loops performed on the same devices, provide direct evidence that gate-voltage modification of the PMA is indeed due to the oxidation of the cobalt layer at the  $\text{Co}/\text{Al}$  interface, driven by the migration of oxygen ions. Moreover, the range of the degree of Co oxidation for which the magnetization is OOP is the same in the gated and reference samples, confirming the origin of the gate-driven manipulation of magnetic anisotropy in  $\text{Pt}/\text{Co}/\text{AlO}_x$  samples.

The fine control of the PMA by magnetoionic effects and the clarification of the underlying mechanisms open the way for the exploration of low-power logic and neuro-morphic spintronic devices.

## ACKNOWLEDGMENTS

We acknowledge support from the Agence Nationale de la Recherche [Projects No. ANR-17-CE24-0025 (TOP-SKY) and No. ANR-19-CE24-0019 (ADMIS)]. This work was supported by the France 2030 government plan managed by the Agence Nationale de la Recherche (project PEPR SPIN CHIREX ANR-22-EXSP-0002). The authors acknowledge funding from the European Union's Horizon 2020 research and innovation program under Marie Skłodowska-Curie Grant Agreements No. 754303 and No. 860060 "Magnetism and the Effect of Electric Field" (MagnEFi). B. Fernandez, T. Crozes, Ph. David, E. Mossang, and E. Wagner are acknowledged for their technical help at the Institut Néel. Stéphane Auffret and Jérôme Faure-Vincent are acknowledged for the deposition of the multilayer samples at SPINTEC. We thank Florian

Godel from Laboratoire Albert Fert for etching the Pt electrodes during our staying at SOLEIL, which allowed us to measure the HAXPES spectra of the gated devices.

C.B. and J.F. contributed equally to this work.

- 
- [1] T. Nozaki, T. Yamamoto, S. Miwa, M. Tsujikawa, M. Shirai, S. Yuasa, and Y. Suzuki, Recent progress in the voltage-controlled magnetic anisotropy effect and the challenges faced in developing voltage-torque MRAM, *Micromachines* **10**, 327 (2019).
- [2] F. Matsukura, Y. Tokura, and H. Ohno, Control of magnetism by electric fields, *Nat. Nanotechnol.* **10**, 209 (2015).
- [3] M. Weisheit, S. Fähler, A. Marty, Y. Souche, C. Poinsignon, and D. Givord, Electric field-induced modification of magnetism in thin-film ferromagnets, *Science* **315**, 349 (2007).
- [4] T. Maruyama, Y. Shiota, T. Nozaki, K. Ohta, N. Toda, M. Mizuguchi, A. A. Tulapurkar, T. Shinjo, M. Shiraishi, and S. Mizukami, Large voltage-induced magnetic anisotropy change in a few atomic layers of iron, *Nat. Nanotechnol.* **4**, 158 (2009).
- [5] Y. Shiota, T. Nozaki, F. Bonell, S. Murakami, T. Shinjo, and Y. Suzuki, Induction of coherent magnetization switching in a few atomic layers of FeCo using voltage pulses, *Nat. Mater.* **11**, 39 (2011).
- [6] U. Bauer, Y. Lide, J. T. Aik, P. Agrawal, S. Emori, H. Tuller, S. van Dijken, and G. Beach, Magneto-ionic control of interfacial magnetism, *Nat. Mater.* **14**, 174 (2015).
- [7] C. Bi, Y. Liu, T. Newhouse-Illige, M. Xu, M. Rosales, J. W. Freeland, O. Mryasov, S. Zhang, S. G. E. te Velthuis, and W. G. Wang, Reversible control of Co magnetism by voltage induced oxidation, *Phys. Rev. Lett.* **113**, 267202 (2014).
- [8] A. Tan, M. Huang, S. Sheffels, F. Büttner, S. Kim, A. Hunt, I. Waluyo, H. Tuller, and G. S. D. Beach, Hydration of gadolinium oxide ( $GdO_x$ ) and its effect on voltage-induced Co oxidation in a Pt/Co/ $GdO_x$ /Au heterostructure, *Phys. Rev. Mater.* **3**, 064408 (2019).
- [9] A. Tan, M. Huang, C. Avci, F. Büttner, M. Mann, W. Hu, C. Mazzoli, S. Wilkins, H. Tuller, and G. S. D. Beach, Magneto-ionic control of magnetism using a solid-state proton pump, *Nat. Mater.* **18**, 35 (2019).
- [10] M. Ameziane, J. Huhtasalo, L. Flajšman, R. Mansell, and S. van Dijken, Solid-state lithium ion supercapacitor for voltage control of skyrmions, *Nano Lett.* **23**, 3167 (2023).
- [11] J. de Rojas, A. Quintana, A. Lopeandía, J. Salguero, B. Muñoz, F. Ibrahim, M. Chshiev, A. Nicolenco, M. Liedke, M. Butterling, A. Wagner, V. Sireus, L. Abad, C. J. Jensen, K. Liu, J. Nogués, J. Costa-Krämer, E. Menéndez, and J. Sort, Voltage-driven motion of nitrogen ions: A new paradigm for magneto-ionics, *Nat. Commun.* **11**, 5871 (2020).
- [12] A. Fassatoui, J. Peña Garcia, L. Ranno, J. Vogel, A. Bernard-Mantel, H. Béa, S. Pizzini, and S. Pizzini, Reversible and irreversible voltage manipulation of interfacial magnetic anisotropy in Pt/Co/oxide multilayers, *Phys. Rev. Appl.* **14**, 064041 (2020).
- [13] A. Fassatoui, L. Ranno, J. Peña Garcia, C. Balan, J. Vogel, H. Béa, and S. Pizzini, Kinetics of ion migration in the electric field-driven manipulation of magnetic anisotropy of Pt/Co/oxide multilayers, *Small* **17**, 2102427 (2021).
- [14] C. Balan, J. Peña Garcia, A. Fassatoui, J. Vogel, D. de Souza Chaves, M. Bonfim, J.-P. Rueff, L. Ranno, and S. Pizzini, Tuning the dynamics of chiral domain walls of ferromagnetic films by magnetoionic effects, *Phys. Rev. Appl.* **18**, 034065 (2022).
- [15] S. Monso, B. Rodmacq, S. Auffret, G. Casali, F. Fettar, B. Gilles, B. Dieny, and P. Boyer, Crossover from in-plane to perpendicular anisotropy in Pt/CoFe/ $AlO_x$  sandwiches as a function of Al oxidation: A very accurate control of the oxidation of tunnel barriers, *Appl. Phys. Lett.* **80**, 4157 (2002).
- [16] B. Dieny and M. Chshiev, Perpendicular magnetic anisotropy at transition metal/oxide interfaces and applications, *Rev. Mod. Phys.* **89**, 025008 (2017).
- [17] A. Manchon, C. Ducruet, L. Lombard, S. Auffret, B. Rodmacq, B. Dieny, S. Pizzini, J. Vogel, V. Uhlir, M. Hochstrasser, and G. Panaccione, Analysis of oxygen induced anisotropy crossover in Pt/Co/ $MO_x$  trilayers, *J. Appl. Phys.* **104**, eid 043914 (2008).
- [18] A. Manchon, S. Pizzini, J. Vogel, V. Uhlir, L. Lombard, C. Ducruet, S. Auffret, B. Rodmacq, B. Dieny, M. Hochstrasser, and G. Panaccione, X-ray analysis of oxygen-induced perpendicular magnetic anisotropy in Pt/Co/ $AlO_x$  trilayers, *J. Magn. Magn. Mater.* **320**, 1889 (2008).
- [19] A. Manchon, S. Pizzini, J. Vogel, V. Uhlir, L. Lombard, C. Ducruet, S. Auffret, B. Rodmacq, B. Dieny, M. Hochstrasser, and G. Panaccione, X-ray analysis of the magnetic influence of oxygen in Pt/Co/ $AlO_x$  trilayers, *J. Appl. Phys.* **103**, 07A912 (2008).
- [20] X. Zhou, Y. Yan, M. Jiang, B. Cui, F. Pan, and C. Song, Role of oxygen ion migration in the electrical control of magnetism in Pt/Co/Ni/ $HfO_2$  films, *J. Phys. Chem. C* **120**, 1633 (2016).
- [21] J. C. Woicik, *Hard X-Ray Photoelectron Spectroscopy (HAXPES)* (Springer, Switzerland, 2006).
- [22] P. Nukala, M. Ahmadi, Y. Wei, S. de Graaf, E. Stylianidis, T. Chakraborty, S. Matzen, H. W. Zandbergen, A. Björling, D. Mannix, D. Carbone, B. Kooi, and B. Noheda, Reversible oxygen migration and phase transitions in hafnia-based ferroelectric devices, *Science* **372**, 630 (2021).
- [23] M. Sicot, S. Andrieu, F. Bertran, and F. Fortuna, Electronic properties of Fe, Co, and Mn ultrathin films at the interface with MgO(001), *Phys. Rev. B* **72**, 144414 (2005).
- [24] M. C. Biesinger, B. P. Payne, A. P. Grosvenor, L. W. Lau, A. R. Gerson, and R. S. Smart, Resolving surface chemical states in XPS analysis of first row transition metals, oxides and hydroxides: Cr, Mn, Fe, Co and Ni, *Appl. Surf. Sci.* **257**, 2717 (2011).
- [25] G. A. Carson, M. H. Nassir, and M. A. Langell, Epitaxial growth of  $Co_3O_4$  on CoO(100), *J. Vac. Sci. Technol. A* **14**, 1637 (1996).